Macromolecules

ARTICLE

pubs.acs.org/Macromolecules

Fluorene-Based Poly(arylene ether sulfone)s Containing Clustered Flexible Pendant Sulfonic Acids as Proton Exchange Membranes†

Chenyi Wang,[‡,∥] Nanwen Li,[‡] Dong Won Shin,[§] So Young Lee,[§] Na Rae Kang,[‡] Young Moo Lee,*[,‡,§] and Michael D. Guiver*[,‡,⊥]

[‡]WCU Department of Energy Engineering, College of Engineering, Hanyang University, Seoul 133-791, Republic of Korea

[§]School of Chemical Engineering, College of Engineering, Hanyang University, Seoul 133-791, Republic of Korea

[⊥]Institute for Chemical Process and Environmental Technology, National Research Council Canada, Ottawa, Ontario K1A 0R6, Canada

[∥]School of Materials Science and Engineering, Changzhou University, Changzhou, 213164, China

ABSTRACT: A new bisphenol monomer, 9,9-bis(3,5-dimethoxy-4-hydroxyphenyl) fluorene, was synthesized and polymerized to form fluorene-based poly(arylene ether sulfone) copolymers containing tetra-methoxy groups (MPAES). After converting the methoxy group to the reactive hydroxyl group, the respective side-chain type sulfonated copolymers (SPAES) were obtained by sulfobutylation. The polymers were characterized by ^{1}H NMR, thermogravimetric analysis (TGA), water uptake, and proton and methanol transport for fuel cell applications. These SPAES copolymers had good overall properties as polymer electrolyte membrane (PEM) materials, having high proton conductivity in the range of 0.061−0.209 and 0.146−0.365 S/cm at 30 and 80 °C (under hydrated conditions), respectively. SPAES-39 (IEC = 1.93 mequiv/g) showed higher or comparable proton conductivity than that of Nafion 117 at 50−95% RH (relative humidity). The methanol permeabilities of these membranes were in the range of 3.22 to 13.1 × 10^{-7} cm^2/s, which is lower than Nafion (15.5 × 10^{-7} cm^2/s). In comparison with some reported sulfonated poly(arylene ether sulfone)s containing pendent sulfophenyl groups, the present fluorene-based SPAES containing clustered flexible pendent aliphatic sulfonic acid groups displayed better properties, such as lower water uptake and higher proton conductivities. A combination of high proton conductivities, low water uptake, and low methanol permeabilities for selected SPAES indicates that they are good candidate proton exchange membrane materials for evaluation in fuel cell applications.

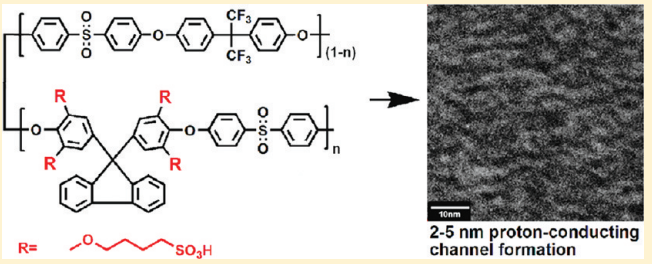

INTRODUCTION

Polymer electrolyte membrane fuel cells (PEMFC) have attracted considerable attention as candidates for alternative power sources due to their high power density, good energy conversion efficiency, and zero emissions levels.[1−4] Perfluorosulfonic acid (PFSA) polymers such as Nafion (DuPont) are the most established and state-of-the-art polymer electrolyte membranes (PEMs) for PEMFC because of their excellent chemical stability and high proton conductivity, but their limited operating temperature range up to 80 °C, high methanol/gas diffusion, environmental recyclability, and high cost are perceived as significant disadvantages. These challenges have driven the investigation of aromatic hydrocarbon polymers as alternative PEM materials.[5−7] The most widely reported aromatic PEMs include sulfonated derivatives of poly(phenylene)s,[8,9] poly(arylene ether ketone)s,[10−12] poly(arylene ether sulfone)s,[13,14] poly(arylene sulfide sulfone)s,[15−17] poly(arylene ether)s,[18,19] and polyimides.[20−25] Generally, the sulfonic acid groups in these polymers are located on the main chain, and the rigid polyaromatic backbone prevents continuous ionic clustering from occurring to form distinct phase-separated structures.[26] As a result, these sulfonated polymers only attain suitable conductivities at high ion exchange capacity (IEC) and high water content, which consequently lead to large dimensional variations and poor mechanical properties. The dimensional stability and proton conductivity of aromatic PEMs are crucial issues that require improvement through careful structural design.

A viable strategy to improve the properties and performance of aromatic PEMs is to design polymer architecture that distinctly separates the hydrophilic sulfonic acid groups from the hydrophobic polymer main chain by locating the sulfonic acid groups on flexible side chains, which may induce improved nanophase separation between hydrophilic and hydrophobic domains.[27] Nafion is a statistical copolymer comprising a highly hydrophobic perfluorinated backbone that contains a number of short, flexible pendant side chains with single strongly hydrophilic sulfonic acid groups. The nanophase-separated structure of Nafion may be responsible for its excellent thermal, mechanical, and electrochemical properties. Currently, several research groups are focusing their work on the development of side-chain

Received: July 12, 2011
Revised: August 9, 2011
Published: August 25, 2011

type sulfonated hydrocarbon-based polymers. Jannasch and co-workers reported a sulfophenoxybenzoyl polysulfone and sulfonaphthaoxybenzoyl polysulfone that was prepared by attaching pendant sulfonated aromatic side chains to polysulfone, showing proton conductivities of 0.11−0.32 S/cm at 120 °C.[28] Jiang and co-workers,[29] Na and co-workers,[30,31] and Zhang and co-workers[32] reported sulfonated aromatic polymers containing one or two pendant sulfoalkyl groups in each hydrophilic unit. The highest conductivity of 0.179 S/cm was obtained for these copolymers (IEC = 1.82 mequiv/g) under a hydrated state at 80 °C, which is higher than that of Nafion 117 (0.146 S/cm).[31] Okamoto and co-workers[33] and Watanabe and co-workers[34] reported two types of SPIs bearing a pendant sulfonic acid group on an aliphatic side chain. Compared with main-chain type SPIs, these side-chain type SPIs exhibited much improved hydrolytic stability and high conductivities. In our previous work, we reported a series of pendant or comb type poly(arylene ether sulfone)s by attaching pendant sulfonated aromatic side chains to the backbone.[35−37] The results also indicated that these side-chain type sulfonated polymers displayed advantageous proton conductivities with relatively low water content.

Another approach to enhance PEM performance can be realized by introducing locally and densely sulfonated structures into the aromatic polymer backbone.[38−41] The large difference in polarity between the locally and densely sulfonated units and hydrophobic units of the polymers results in the formation of well-defined nanophase-separated structures and can induce efficient proton conduction. Hay and co-workers reported the synthesis of linear poly(sulfide ketone)s and branched poly(ether ketone)s bearing clusters of six sulfonic acid moieties situated on the chain ends, by regioselective postsulfonation.[38,39] These ionomers possessed good microphase-separated morphology and displayed relatively high proton conductivity (0.091 S/cm at room temperature with 100% RH (relative humidity)) at very low IEC (1.09 mequiv/g). However, it is difficult to further increase their IEC values and proton conductivity based on this methodology because the sulfonated groups are located only on the chain ends. Ueda and co-workers reported locally sulfonated poly(ether sulfone)s with 10 sulfonic acid groups in each repeating unit by postsulfonation with sulfuric acid.[40,41] The sulfonated polymers (IEC = 1.96−2.38 mequiv/g) exhibited good proton conductivity under low humidity conditions, which is comparable to the proton conductivity of Nafion 117 over a wide range of RH. Densely sulfonated segmented poly(arylene ether sulfone)s showed nanophase separation of hydrophilic and hydrophobic blocks.[42]

Over the past few years, much research focus has been on fluorene-based sulfonated poly(arylene ether)s.[43−49] It has been demonstrated that fluorene-based PEMs show some attractive properties, not only for chemical, thermal, and mechanical stability, but also good proton conductivities and fuel cell performance over several thousand hours.[46] Herein, we introduce a new fluorene-based bisphenol monomer and derived sulfonated poly(arylene ether sulfone) copolymers containing clusters of four butylsulfonic acid units per repeat unit along the main chain. To the best of our knowledge, this is the first reported example of fluorene-based PEMs containing locally and densely populated flexible butylsulfonic acid pendant units. The synthesis and properties of this new series of PEMs are investigated and compared with a previously reported side-chain type poly(arylene ether sulfone)s containing pendant sulfophenyl groups.

EXPERIMENTAL SECTION

Materials. 2,6-Dimethoxyphenol, 9-fluorenone, mercaptopropionic acid (MPA), 4,4′-(hexafluoroisopropylidene)diphenol (6F-BPA), boron tribromide (BBr_3), 1,4-butanesultone, and bis(4-fluorophenyl)sulfone were purchased from Sigma-Aldrich. *N*-Methyl-2-pyrrolidone (NMP), dimethyl sulfoxide (DMSO), and all other solvents and reagents were reagent grade and were used as received.

9,9-Bis(3,5-dimethoxy-4-hydroxyphenyl)fluorene (DMHF). To a 250 mL four-necked round-bottom flask, equipped with a reflux condenser, magnetic stirrer, nitrogen inlet, thermometer, and a drop funnel, 7.20 g (0.04 mol) of 9-fluorenone, 15.42 g (0.1 mol) of 2,6-dimethoxyphenol, 0.1 mL of MPA, and 10 mL of toluene were introduced. The reaction mixture was stirred under nitrogen atmosphere at 30 °C for 30 min. A portion of 1.5 mL of 98 wt % H_2SO_4 was then added dropwise in 10 min, and the temperature was thereafter raised to 55 °C for 4−6 h with stirring. When the reaction mixture became solid, it was cooled down and transferred into cold water. Light yellow solid product was obtained by filtration. Crude product was recrystallized from toluene twice to afford 10.54 g (yield: 56%) of pure white crystalline 9,9-bis(3,5-dimethoxy-4-hydroxyphenyl)fluorene, mp: 186−187 °C. ^{1}H NMR (300 MHz, DMSO-d_6; ppm): 8.34 (s, 2H, −OH), 7.90 (d, J = 7.2, 2H, H_a), 7.50 (d, J = 7.2, 2H, H_d), 7.40 (t, J = 7.5, 2H, H_b), 7.30 (t, J = 7.5, 2H, H_c), 6.31 (s, 4H, H_e), 3.53 (s, 12H, $-OCH_3$).

Synthesis of Poly(arylene ether sulfone)s Containing Methoxy Groups (MPAES-*xx*). A typical synthetic procedure, illustrated by the preparation of MPAES-39 copolymer (xx: DMHF/6F-BPA = 39:61), is described as follows. Samples of 1.101 g (2.34 mmol) of DMHF, 1.231 g (3.66 mmol) of 6F-BPA, 1.526 g (6 mmol) of bis(4-fluorophenyl)sulfone, 1.076 g (7.8 mmol) of K_2CO_3, 16 mL of NMP, and 8 mL of toluene were added into a 100 mL three-neck flask equipped with a mechanical stirrer, a Dean−Stark trap, and a nitrogen inlet. The solution was allowed to reflux at 140 °C, while the water was azeotropically removed from the reaction mixture. After 4 h, the toluene was removed from the reaction by slowly increasing the temperature to 155 °C, and then the reaction was allowed to continue for another 5−8 h. After the reaction, 5 mL of NMP was added to the mixture to reduce the solution viscosity. The solution was poured into 500 mL of deionized water with vigorous stirring. The resulting fibrous copolymer was washed with deionized water and hot methanol several times and dried at 100 °C under vacuum for 24 h.

Conversion of a Methoxy Group (MPAES-*xx*) to a Hydroxyl Group (HPAES-*xx*). A sample of 2.0 g of MPAES-39 was dissolved into 50 mL of CH_3Cl in a 100 mL three-neck flask equipped with a mechanical stirrer and a nitrogen inlet. BBr_3 (2 mL) was mixed with CH_3Cl (20 mL), and the resulting solution was added dropwise to the MPAES-39 solution at 0 °C (ice bath). After 6 h, the resulting copolymer (HPAES-39) was filtered, washed with boiling water, recovered, and then dried under vacuum at 100 °C for 24 h.

Preparation of Sulfonated Copolymer (SPAES-*xx*). Samples of 2.0 g of HPAES-39 and 0.60 g of NaOH were dissolved into 30 mL of DMSO at room temperature and stirred for 10 min under nitrogen atmosphere. Then 2 mL of 1,4-butanesultone was added, and the reaction was heated to 100 °C for another 6 h. The viscous solution was precipitated into 500 mL of isopropanol and washed with boiling water several times before being dried under vacuum at 100 °C for 24 h.

Membrane Preparation. The dried sulfonated copolymers were readily dissolved as 10−15 wt % solutions in DMSO at 60 °C. The solutions were filtered and cast onto glass plates and left to dry and then treated in vacuum at 60 °C for 20 h. The membranes were immersed into 2.0 M H_2SO_4 solution for 24 h and then washed in deionized water for another 24 h to obtain the H^+ form membranes.

Measurements. ^{1}H NMR spectra were measured on a 300 MHz Bruker AV 300 spectrometer using DMSO-d_6 or $CDCl_3$ as solvent. The

inherent viscosities were determined on 0.5 g dL^{-1} concentration of polymer in NMP with an Ubbelohde capillary viscometer at 30 ± 0.1 °C. The thermogravimetric analyses (TGA) were obtained in nitrogen with a Perkin-Elmer TGA-2 thermogravimetric analyzer at a heating rate of 10 °C/min. The gel permeation chromatographic (GPC) analysis was carried out with Tosoh HLC-8320 instrument (tetrahydrofuran as eluent and polystyrene as standard).

The oxidative stability of the membranes was tested by immersing the films into Fenton's reagent (3% H_2O_2 containing 2 ppm $FeSO_4$) at 80 °C. The retained weights (RW) of membranes after treatment in Fenton's reagent for 1 h, and the dissolution time (t) of polymer membranes into the reagent, were used to evaluate the comparative oxidative resistance.

The proton conductivity (σ, S/cm) of each membrane coupon (size: 1 cm × 4 cm) was obtained using $\sigma = d/L_sW_sR$ (d: distance between reference electrodes, and L_s and W_s are the thickness and width of the membrane, respectively). The resistance value (R) was measured over the frequency range from 100 mHz to 100 kHz by four-point probe alternating current (ac) impedance spectroscopy using an electrode system connected with an impedance/gain-phase analyzer (Solartron 1260) and an electrochemical interface (Solartron 1287, Farnborough, Hampshire, UK). The membranes were sandwiched between two pairs of gold-plate electrodes. The membranes and the electrodes were set in a Teflon cell, and the distance between the reference electrodes was 1.0 cm. Conductivity measurements under fully hydrated conditions were carried out in a thermo-controlled chamber with the cell immersed in liquid water.

The methanol permeability was determined by using a cell consisting of two-half-cells separated by the membrane, which was fixed between two rubber rings. Methanol (2 M) was placed on one side of the diffusion cell, and water was placed on the other side. Magnetic stirrers were used on each compartment to ensure uniformity. The concentration of the methanol was measured by using a Shimadzu GC-1020A series gas chromatograph. Peak areas were converted into methanol concentration with a calibration curve. The methanol permeability was calculated by the following equation:

$$C_B(t) = \frac{A}{V_B}\cdot\frac{DK}{L}\cdot C_A\cdot(t - t_0) \quad (1)$$

where C_A and C_B are the methanol concentrations of feed side and permeated through the membrane, respectively. A, L, and V_B are the effective area, membrane thickness, and the liquid volume of permeate compartment, respectively. DK is defined as the methanol permeability. t_0 is the time lag.

Characterization Methods. The membrane density was measured from a known membrane dimension and weight after drying at 100 °C for 24 h. Water uptake was measured after drying the membrane in acid form at 100 °C under vacuum overnight. The dried membrane was immersed in water at 30 °C and periodically weighed on an analytical balance until a constant water uptake weight was obtained. Then, the volume-based water uptake (WU) was obtained. A volume-based IEC (IEC_v) was obtained by multiplying the membrane density by the IEC_w values which were estimated from the copolymer structure. This calculation resulted in IEC_v (dry) based on the dry membrane density. An IEC_v (wet) was then calculated based on membrane water uptake.[35,50] For transmission electron microscopy (TEM) observations, the membranes were stained with lead ions by ion exchange of the sulfonic acid groups in 0.5 M lead acetate aqueous solution, rinsed with deionized water, and dried in vacuum oven for 12 h. The stained membranes were embedded in epoxy resin, sectioned to 70 nm thickness with a RMCMTX Ultra microtome, and placed on copper grids. Electron micrographs were taken with a Carl Zeiss LIBRA 120 energy-filtering transmission electron microscope using an accelerating voltage of 120 kV.

Scheme 1. Synthesis of the Monomer DMHF

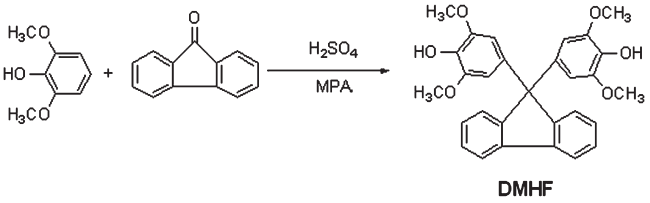

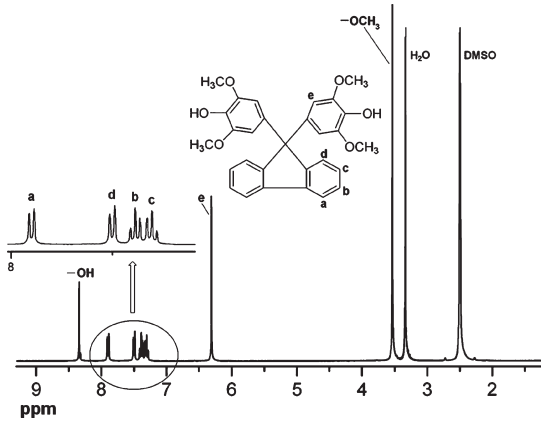

Figure 1. ^{1}H NMR spectrum of bisphenol monomer DMHF.

RESULTS AND DISCUSSION

Synthesis and Characterization of the Monomers and Polymers. The monomer DMHF was synthesized by reacting 9-fluorenone with 2,6-dimethoxyphenol, by a phenol condensation reaction catalyzed by MPA and sulfuric acid. Scheme 1 shows the synthesis of monomer DMHF; the structure was confirmed by ^{1}H NMR spectroscopy in DMSO-d_6. As shown in Figure 1, the −OH signal appeared at 8.34 ppm, and the signals at 3.53 ppm correspond to $-OCH_3$. The clean spectrum of aromatic protons H_a to H_e confirms the structure of the new monomer DMHF.

Poly(arylene ether sulfone) copolymers containing methoxy groups (MPAES-*xx*, xx: mole ratio (%) of DMHF) were synthesized by polycondensation using various feed ratios of DMHF/HFDP, resulting in copolymers with different molar percentages of pendant groups, as shown in Scheme 2. The polymerization reactions proceeded smoothly to high molecular weight (M_n > 50 000 g/mol), and no cross-linking was evident when the temperature was controlled by an oil bath (less than 165 °C) and the reaction time was less than 10 h, because the methoxy groups are not reactive under these conditions. Table 1 shows the molecular weight, polydispersity index, and inherent viscosity of MPAES-*xx* copolymers.

The conversion of the $-OCH_3$ to reactive −OH for grafting was conducted using BBr_3 in chloroform. Although the MPAES-*xx* copolymers were readily soluble in chloroform, the resulting HPAES-*xx* copolymers (containing −OH) were insoluble due to the polar nature of the −OH group. The conversion of MPAES-*xx* to HPAES-*xx* copolymer (Scheme 2) resulted in precipitation from chloroform. Comparative ^{1}H NMR spectra of the MPAES-*xx* ($-OCH_3$) and HPAES-*xx* copolymers (−OH) confirmed that complete demethylation occurred; $-OCH_3$ proton signals

Scheme 2. Synthesis of Copolymers MPAES-*xx*, HPAES-*xx*, and SPAES-*xx*

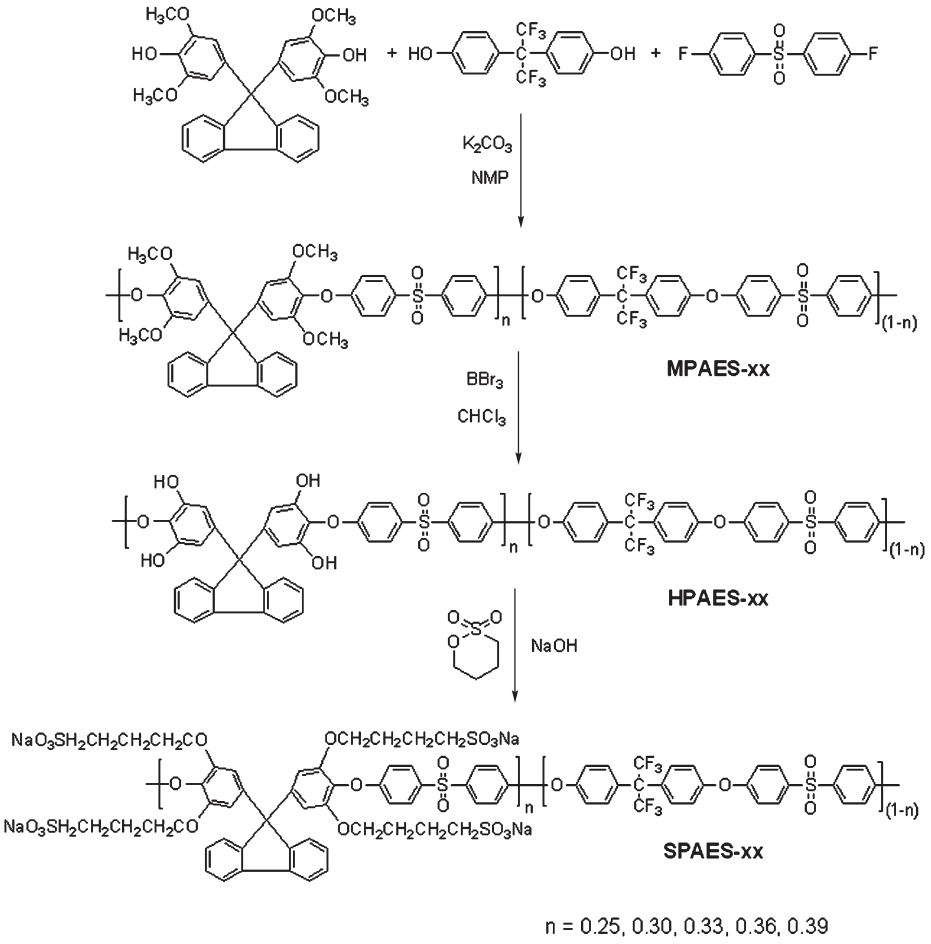

Table 1. Molecular Weights and Inherent Viscosities of MPAES-*xx* Copolymers

copolymers	M_n[a] (10^4 g/mol)	M_w (10^4 g/mol)	PDI	η_{inh}[b] (dL/g)
MPAES-25	6.12	15.97	2.61	0.64
MPAES-30	7.01	19.49	2.78	0.71
MPAES-33	7.28	19.65	2.70	0.73
MPAES-36	5.43	11.08	2.04	0.58
MPAES-39	6.83	15.09	2.21	0.66

[a] Measured at 30 °C using THF as a solvent and polystyrene as a standard. [b] 0.5 g/dL in NMP at 30 °C.

at 3.48 ppm disappeared, and −OH proton signals appeared at 9.43 ppm, as shown in Figure 2.

A variety of side-chain type PEMs containing one or two pendant sulfoalkyl groups in each hydrophilic unit have been prepared by the direct copolymerization method[29,33,34] or by chemically grafting the pendants onto polymers.[30−32] Compared to chemical grafting, the direct copolymerization method allows close control of sulfonation content and the polymer structure. However, the synthesis and purification of sulfonated monomers may be complicated and difficult, especially for those containing a high content of sulfonic groups. The chemical grafting method avoids the need to prepare sulfonated monomers and offers an easier route to introduce locally and densely populated sulfonated structures into the aromatic polymer backbone. Hvilsted and co-workers recently demonstrated that the parent polymers containing hydroxyl groups in the para-position of the aromatic ring could be sulfopropylated through a nucleophilic ring-opening reaction with 1,3-propanesultone using NaOH.[51] Na and co-workers also prepared a series of sulfonated poly(arylene ether ketone)s by the same method through hydroxyl groups in the ortho-positon of the aromatic ring grafting and with 1,4-butanesultone using NaOH.[31] In the present work, we applied this synthetic method. Scheme 2 shows the grafting reaction of sulfobutyl groups onto HPAES-*xx* by a nucleophilic ring-opening reaction with 1,4-butanesultone using NaOH. A series of polymers with different butylsulfonate contents were obtained by adjusting the −OH content in HPAES-*xx* copolymers, which were reacted with excess 1,4-butanesultone and NaOH. The sulfonated polymer series were readily soluble in DMSO and NMP and afforded flexible and transparent films by polymer solution casting. The chemical structures of SPAES-*xx* were confirmed by ^{1}H NMR spectra (Figure 3). As expected, the −OH proton signal at 9.43 ppm disappeared, while the signals for the four sulfobutyl methylene groups (H_j, H_k, H_l, and H_m) appeared at lower frequencies. Interestingly, the proton of H_e appeared as a broad multiplet, because the steric hindrance of the bulky sulfobutyl groups prevents rotational freedom of the benzene ring, which further supports the formation of SPAES-*xx* bearing sulfobutyl groups.

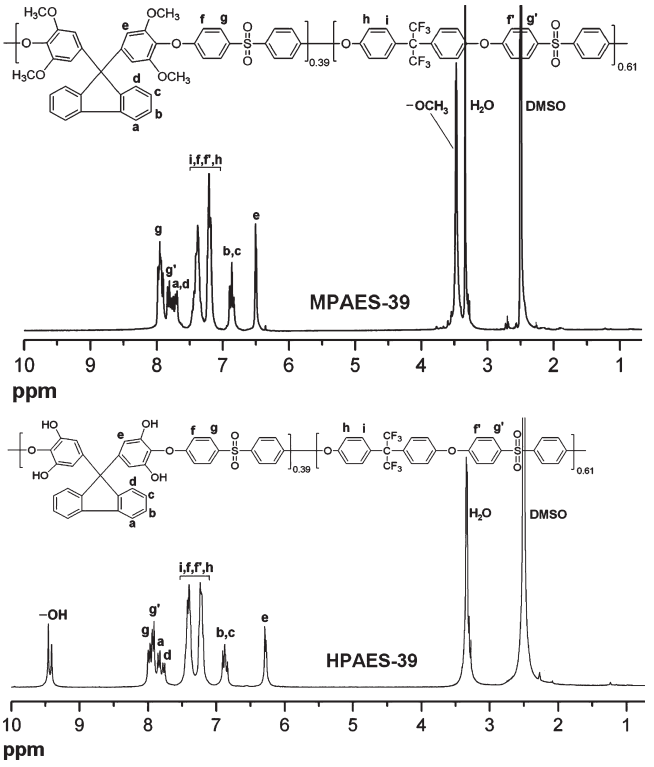

Figure 2. Comparative ^{1}H NMR spectra of the MPAES-39 (−OCH_3) and HPAES-39 (−OH) copolymers.

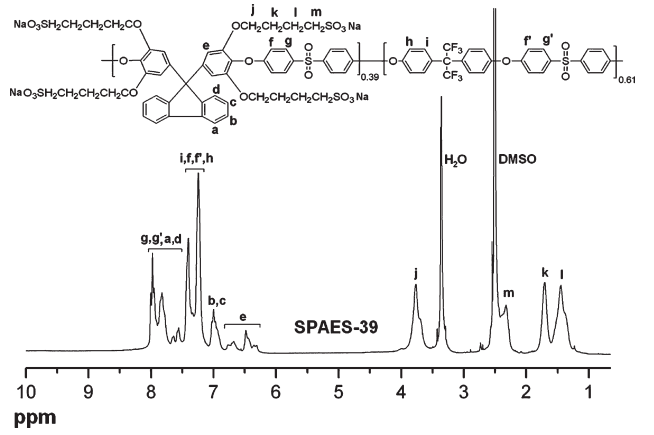

Figure 3. ^{1}H NMR spectrum of SPAES-39.

Thermal and Mechanical Properties. The thermal stabilities of the polymers were investigated by TGA, and the 5% weight loss temperatures are listed in Table 2. Figure 4 shows the TGA curves of SPAES-*xx* in the sulfonic acid form, which appear to have three distinct degradation steps. The initial degradation step observed at around 220−330 °C is likely associated with the thermal degradation of the (sulfo)butoxy groups, while the second and third steps starting at about 370 °C correspond to the remainder of the polymer.

The mechanical properties of the membranes are listed in Table 2. The SPAES membranes in 40% RH and 80 °C had tensile moduli in the range of 0.83−1.23 GPa, elongations at break of 16.7−34.1%, and tensile strength at break of 36.9−52.8 MPa. In the dry state, the samples also showed good mechanical properties with tensile moduli of 1.24−1.92 GPa, elongations at break of 9.3−14.3%, and tensile strength at break of 43.6−61.3 MPa. These results indicate that the side-chain type SPAES membranes were sufficiently tough and ductile for potential use as PEM materials in a fuel cell.

Table 2. Thermal and Mechanical Properties

copolymers	$T_{d5\%}$ (°C)[a]	tensile strength at break (MPa)	Young's modulus (GPa)	elongation at break (%)
SPAES-25	292	52.8 (58.8)[b]	1.23 (1.92)	34.1 (9.3)
SPAES-30	250	49.5 (61.3)	1.22 (1.88)	24.3 (9.7)
SPAES-33	250	48.7 (53.4)	1.12 (1.64)	27.4 (12.0)
SPAES-36	242	49.4 (50.1)	0.99 (1.48)	18.2 (14.3)
SPAES-39	237	36.9 (43.6)	0.83 (1.24)	16.7 (12.2)

[a] 5% weight loss temperature in N_2 gas (acid form membrane). [b] Dry sample values in parentheses.

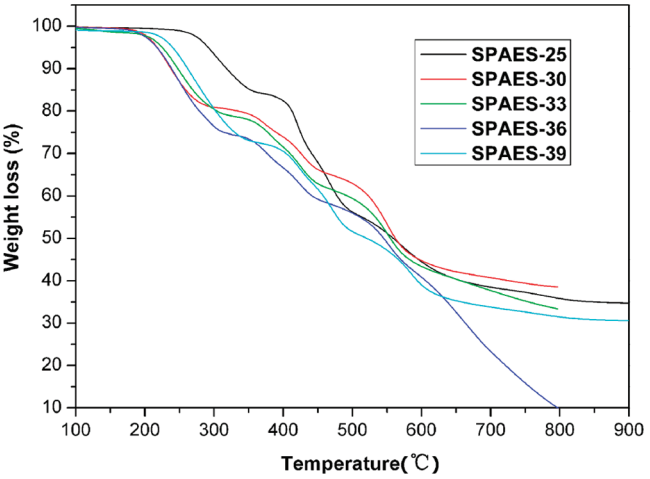

Figure 4. TGA curves of SPAES-*xx* (acid form) membranes from a measurement run at 10 °C/min in N_2.

IEC, Water Uptake, Swelling Ratio, and Oxidative Stability. IEC represents the amount of exchangeable protons in ionomer membranes. The IEC values from titration tests were in the range 1.36−1.93 mequiv/g, which were close to the theoretical values, indicating close to quantitative reaction yields for methoxy conversion and sulfobutylation.

Water uptake (weight- and volume-based) of PEMs is an important parameter for IEC, proton conductivity, dimensional stability, mechanical strength, and membrane-electrode compatibility. Although weight-based IECs (IEC_w) are most often reported, a more realistic comparison of water uptake among different membranes is achieved by using volumetric IECs (IEC_v, mequiv/cm^3), which is defined as the molar concentration of sulfonic acid groups per unit volume containing absorbed water. Table 3 compares the density, IEC, and water uptake (weight- and volume-based) of the copolymer membranes and Nafion. The water uptake of SPAES-*xx* increased with IEC_w and IEC_v (dry), due to the increased hydrophilicity, as shown in Figure 5a, b. The volume-based IEC_v data in Figure 5b shows a very similar trend as the weight-based IEC_w data in Figure 5a. The highest water uptake (wt %) and water uptake (vol %) was 70% and 111% at 80 °C for the highest IEC_w membrane SPAES-39 (IEC_w = 1.93), respectively, which was nearly twice that of

Table 3. IEC, Density, and Water Uptake of the SPAES-*xx* and Nafion Membranes

	IEC_w (mequiv/g)			IEC_v[b] (mequiv/cm^3)		water uptake			
						wt %[c]		vol %[d]	
copolymers	calcd	expt[a]	density (g/cm^3)	dry	wet	30 °C	80 °C	30 °C	80 °C
SPAES-25	1.42	1.36	1.46	1.99	1.81	6.7	16.5	9.8	24.1
SPAES-30	1.63	1.61	1.54	2.48	2.00	15.4	30.4	23.7	46.8
SPAES-33	1.75	1.70	1.56	2.65	2.02	20.2	35.8	31.5	55.8
SPAES-36	1.86	1.86	1.57	2.92	2.08	25.6	46.8	40.2	73.5
SPAES-39	1.97	1.93	1.58	3.05	2.06	30.5	70.3	48.2	111.1
Nafion 117		0.90	1.98	1.78	1.30	18.5	30.6	36.6	60.6

[a] Determined by acid−base titration. [b] Based on volume of dry and/or wet membranes (IEC_v(wet) = IEC_v(dry)/(1 + 0.01WU)). [c] WU (wt %) = $(W_{wet} - W_{dry})/W_{dry} \times 100$. [d] WU (vol %) = $((W_{wet} - W_{dry})/\delta_w)/(W_{dry}/\delta_m) \times 100$. ($W_{wet}$ and W_{dry} are the weights of the wet and dry membranes, respectively; δ_w is the density of water (L g/cm^3), and δ_m is the membrane density in the dry state.)

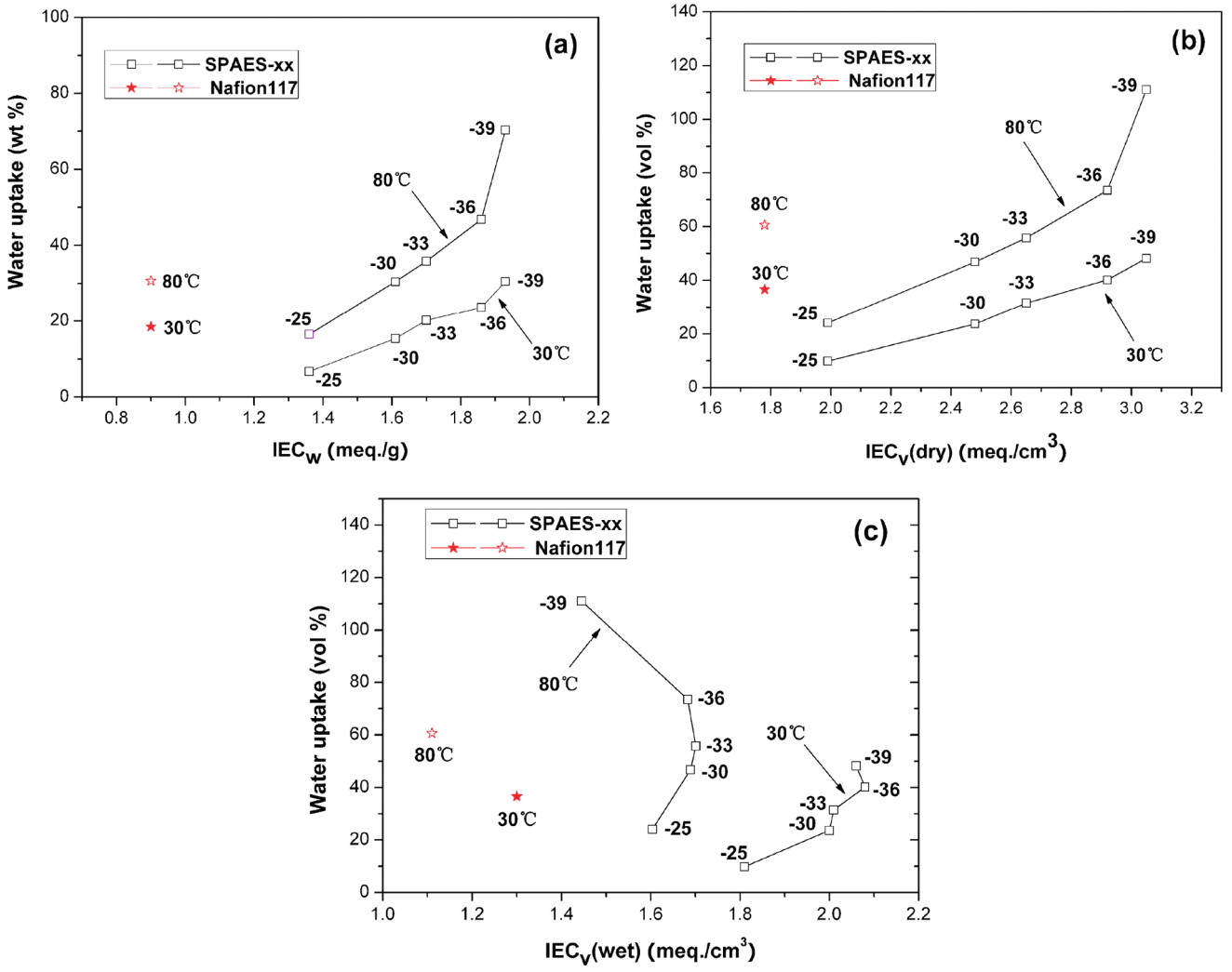

Figure 5. Water uptake dependence of IEC (IEC_w), IEC_v (dry), and IEC_v (wet) values of SPAES-*xx* membranes.

Nafion membrane. The water uptake of the SPAES-*xx* series increased quasilinearly up to SPAES-36 (IEC_w = 1.86) and then dramatically increased at SPAES-39, similar to that reported for comb-shaped sulfonated PEMs in the literature and related to a percolation threshold.[37]

The IEC_v (wet) reflects the concentration of ions within the polymer matrix under hydrated conditions, without distinguishing between those protons that are mostly associated with the sulfonic acid groups and those that are fully dissociated. The IEC_v (wet) of SPAES-*xx* increased from 1.81 to 2.08 mequiv/cm^3 with

dx.doi.org/10.1021/ma2015968 |*Macromolecules* 2011, 44, 7296–7306

the corresponding increase of IEC_w from 1.36 to 1.86 mequiv/g at 30 °C. However, the IEC_v (wet) of SPAES-39 was lower than that of SPAES-36, because the hydration of SPAES-39 resulted in excessive swelling and dilution of the ion concentration after equilibration with water. This is observed in Figure 5c whereby the slope of the 30 and 80 °C curves assumes a reverse direction due to high water uptake (vol %) and reduced IEC_v (wet).

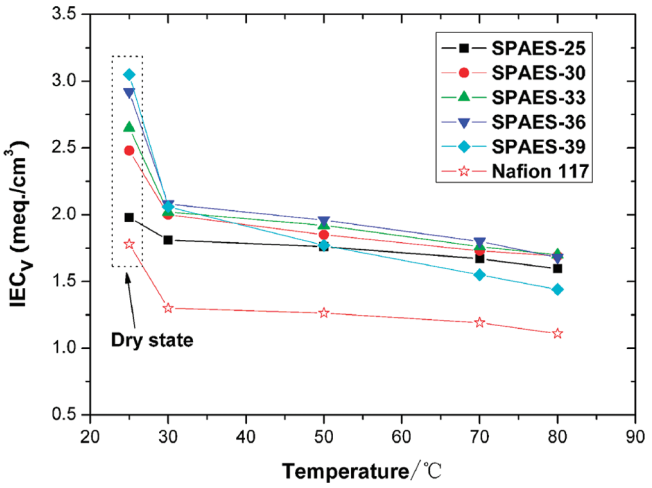

Figure 6. Volumetric IEC_v of SPAES-*xx* and Nafion 117 in water as a function of temperature.

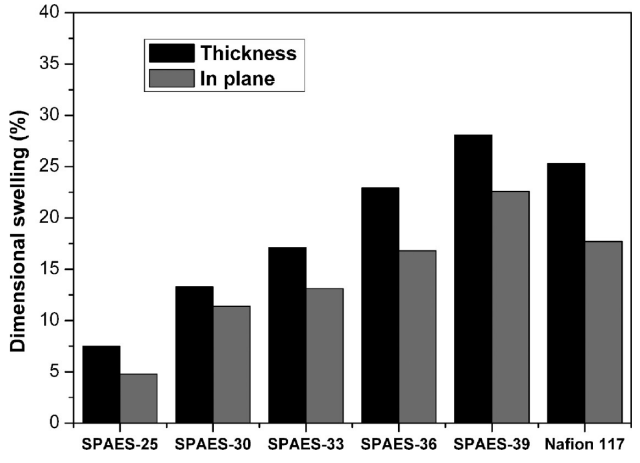

Figure 7. Dimensional swelling of SPAES-*xx* membranes and Nafion 117 at 80 °C.

The IEC_v is plotted as a function of temperature in Figure 6. Similar to Nafion, the IEC_v values decrease with increasing temperature due to increased water volume within the polymer matrix. These side-chain type membranes displayed higher IEC_v than that of Nafion membranes over the temperature range investigated. The SPAES-25 membrane showed approximately the same trend in IEC_v values as Nafion, since the differences in gravimetric IEC were counterbalanced by the differences in density (1.98 g/cm^3 for Nafion and 1.46 g/cm^3 for SPAES-25). The IEC_v (wet) of SPAES-39 membrane with the highest IEC_w decreased sharply at elevated temperatures, to values lower than others at 80 °C, which indicated that this membrane underwent excessive swelling in water.

Figure 7 compares the dimensional swelling ratio of SPAES-*xx* and Nafion in the through-plane and in-plane direction at 80 °C. Besides SPAES-39, all of the SPAES PEMs exhibited a lower dimensional swelling ratio than that of Nafion (Table 4). The side-chain type SPAES-*xx* membranes showed generally a lower swelling ratio than many main-chain type sulfonated poly(arylene ether)s with similar IEC values.[10,11,49] Compared with main-chain type SPAES, the side-chain type SPAES having sulfonic acid units on long flexible side chains may be more effective in suppressing the swelling behavior of the polymer films by inducing hydrophobic and hydrophilic domain phase separation. In addition, the fluorene-based SPAES-*xx* displayed mildly anisotropic membrane swelling, in which the dimensional change was larger in thickness direction than in plane; all of the PEMs except that with the highest IEC had lower dimensional swelling than Nafion 117.

The oxidative stability of the polymers was evaluated in Fenton's reagent at 80 °C. This method is regarded as one of the standard tests to gauge relative oxidative stability and to simulate accelerated fuel cell operating conditions. All of the polymer films exhibited good oxidative stability, as shown in Table 4. Weight retention for all samples was above 93% after treatment in Fenton's reagent at 80 °C for 1 h, and most samples remained undissolved in Fenton's reagent within 2.0 h of treatment at 80 °C, comparable to reported side-chain type PEMs with pendant sulfophenyl groups.[52]

Proton Conductivity and Methanol Permeability. Proton conductivities of the SPAES-*xx* PEMs measured in the RH range of 40−100% at different temperatures are listed in Table 4. Figure 8 shows the proton conductivities as a function of temperature at 100% RH. The proton conductivities of SPAES-*xx*

Table 4. Dimensional Swelling, Proton Conductivity, and Methanol Permeability of the SPAES-*xx* Membranes

	dimensional swelling (%)											
	Δ*t* (thickness)		Δ*l* (in plane)		oxidative stability		proton conductivity in water (S/cm)		proton conductivity (S/cm) (at 80 °C)		methanol permeability (10^{-7} cm^2/s)	relative selectivity
copolymers	30 °C	80 °C	30 °C	80 °C	RW[a] (%)	*t*[b] (h)	30 °C	80 °C	RH 95%	RH 50%		
SPAES-25	2.7	7.5	1.9	4.8	97	4	0.061	0.146	0.061	0.0031	3.22	3.81
SPAES-30	5.1	13.3	3.6	11.4	96	3.5	0.110	0.187	0.107	0.0051	6.64	3.33
SPAES-33	7.3	17.1	5.4	13.1	96	3.5	0.135	0.250	0.130	0.0055	7.05	3.85
SPAES-36	9.1	22.9	7.6	16.8	94	2.5	0.176	0.318	0.206	0.0131	8.06	4.40
SPAES-39	13.9	28.1	12.7	22.6	93	2	0.209	0.365	0.223	0.0160	13.10	3.21
Nafion 117	12.7	25.3	11.6	17.7	98	>6	0.077	0.165	0.131	0.0160	15.50	1.00

[a] Retained weights of membranes after treating in Fenton's reagent for 1 h. [b] Dissolution time of polymer membranes.

dx.doi.org/10.1021/ma2015968 |*Macromolecules* 2011, 44, 7296–7306

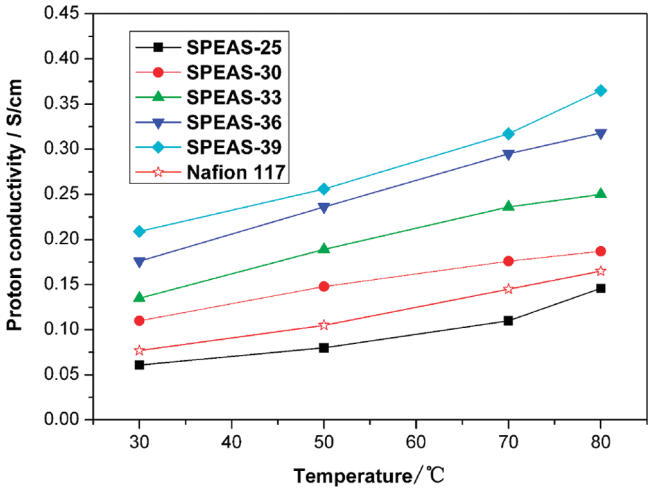

Figure 8. Proton conductivity of SPAES-*xx* membranes and Nafion 117 at different temperatures under fully hydrated conditions.

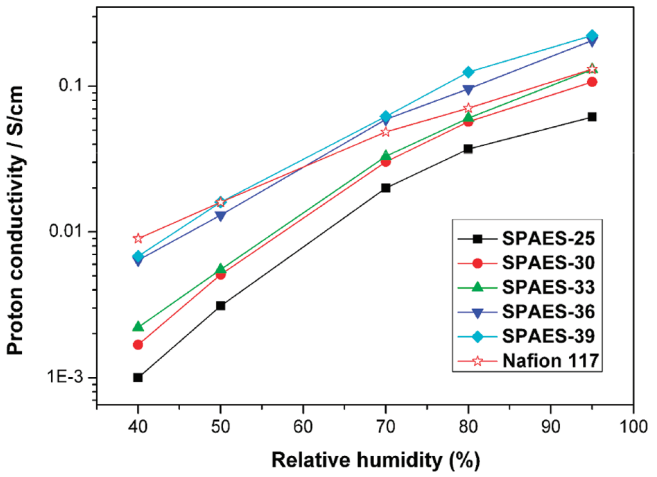

Figure 9. Proton conductivity of SPAES-*xx* membranes and Nafion 117 at 80 °C as a function of RH.

(IEC_w > 1.61) are higher than that of Nafion and increased with temperature. In comparison with similar IEC value side-chain-type sulfonated PEMs containing only two aliphatic sulfonic acid groups per repeat unit (IEC_w = 1.72, σ = 0.114), the present SPAES-33 show much higher proton conductivities (IEC_w = 1.70, σ = 0.250), which indicates that more densely populated aliphatic sulfonic acid groups along the polymer chain appear to be more effective in proton conduction.[31] Figure 9 shows the RH dependence of proton conductivities at 80 °C. As expected, all of the films exhibited increased proton conductivities with increasing RH. SPAES-39 and SPAES-36 showed the highest proton conductivity values, which were comparable to or even higher than that of Nafion at ≥50% RH.

Nonfluorinated randomly sulfonated PEMs generally require high IEC values to attain high proton conductivity because of lower acidity and side-chain flexibility of the sulfonic acid groups and smaller hydrophilic/hydrophobic differences compared to Nafion. In the SPAES-*xx* copolymers, the incorporation of clusters of flexible side-chain sulfonic acid groups could be beneficial to aggregate the ionic clusters, which would lead to more

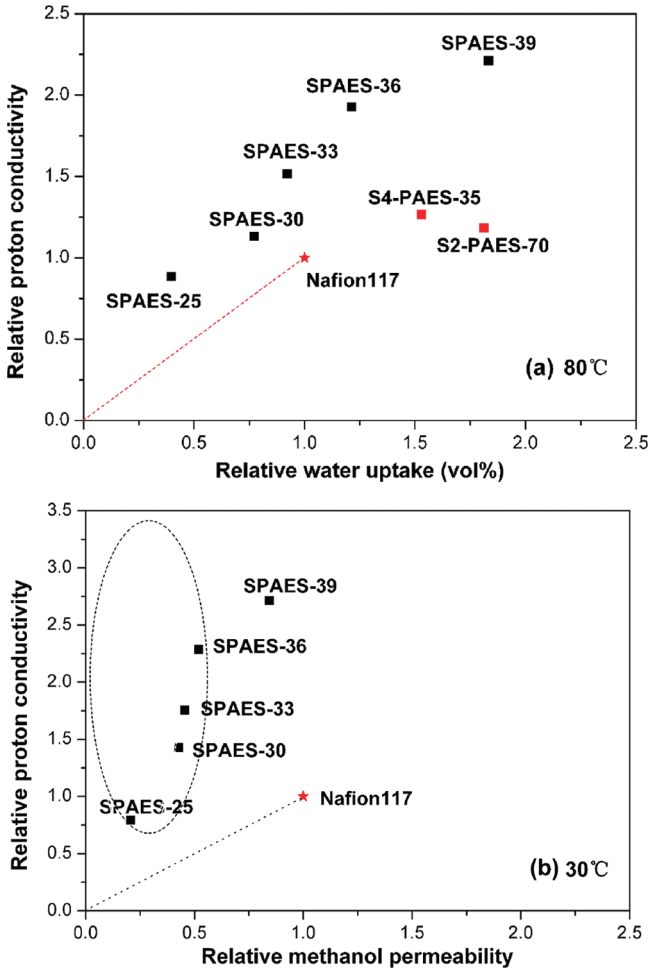

Figure 10. (a) Relative water uptake as a function of relative proton conductivity. (b) Relative proton conductivity as a function of relative methanol permeability.

obvious hydrophilic/hydrophobic separation and improve proton conductivity.

Figure 10a shows the relative water uptake (vol %) as a function of relative proton conductivity. For comparison, the properties of some other side-chain type poly(arylene ether sulfone)s (S2-PAES-70 and S4-PAES-35) containing pendant sulfophenyl groups[35] are also shown in Figure 10a. It should be noted that high relative water uptake and dimensional swelling can lead to difficulties in MEA fabrication, membrane-electrode interfacial resistance, and membrane creep and deformation. On the other hand, conductivity values below 0.05 S/cm can lead to significant ohmic losses under fuel cell operation, since a minimum membrane thickness is often practically limited due to membrane fabrication or mechanical properties. In comparison with S2-PAES-70 (IEC_w = 1.84) and S4-PAES-35 (IEC_w = 1.82) in our previous study,[35] SPAES-36 exhibited a much higher relative proton conductivity and lower relative water uptake. This further indicates that the present approach of introducing multiple flexible sulfonic acid groups onto the fluorine-cardo structure is effective in improving the properties of PEMs.

The membrane properties of SPAES were also investigated for their potential use in direct methanol fuel cells (DMFC). Methanol permeability through the PEM often follows a similar relationship to proton conductivity; that is, the proton conductivity

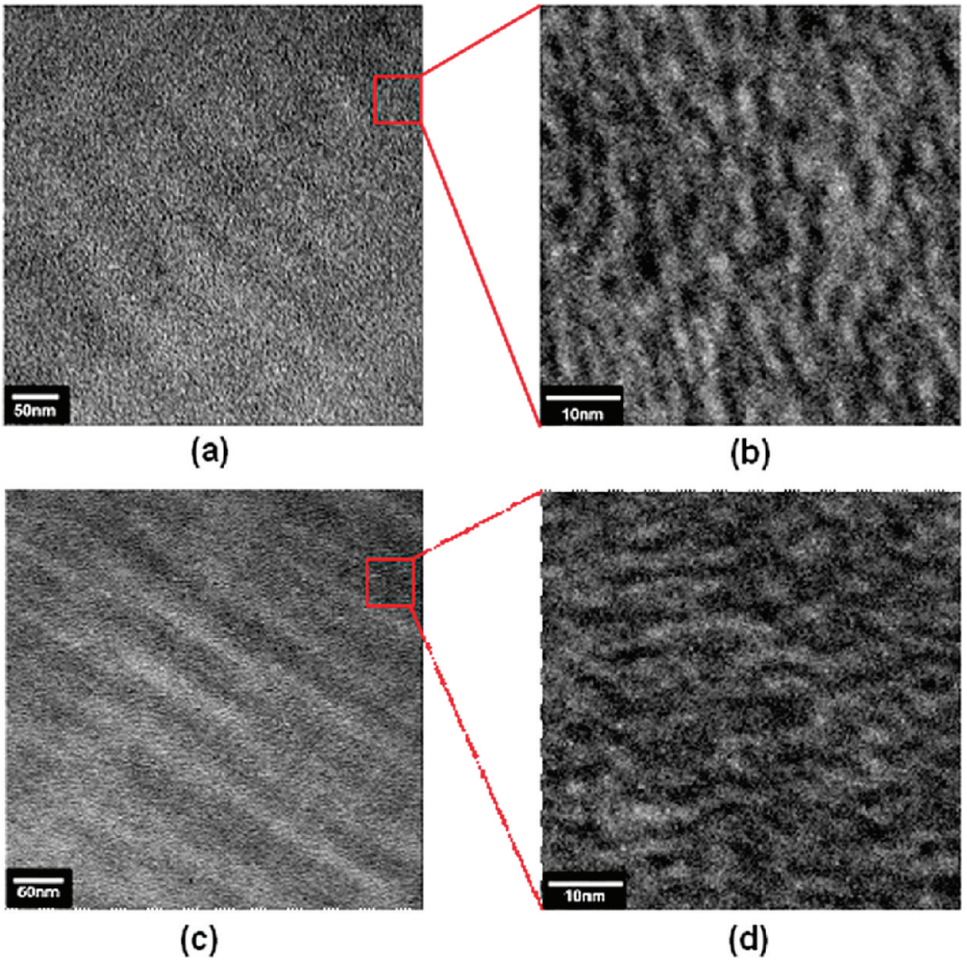

Figure 11. TEM photographs of (a and b) SPAES-33 membrane and (c and d) SPAES-39 membrane.

has a strong trade-off relationship with the methanol permeability. Target membranes suitable for DMFC are ideally located in the upper left-hand corner, as shown by the dotted circle, that is, high conductivity and low methanol permeability. As shown in Figure 10b, SPAES-27, SPAES-30, SPAES-33, and SPAES-36 are located in this target area. Membranes intended for DMFC must have both high proton conductivity and be effective barriers for methanol crossover from the anode to the cathode compartment. Nafion has good proton conductivity due to a strongly interconnected ionic domain structure but it also has high methanol permeability. The present SPAES exhibited low methanol permeability, with values for 10% methanol concentration at room temperature in the range of 3.22×10^{-7} to 13.1×10^{-7} cm^2/s, which is lower than the value for Nafion of 15.5×10^{-7} cm^2/s. Although SPAES-25 has a lower proton conductivity and higher IEC_v than Nafion, it has the potential to achieve improved DMFC performance through its low methanol permeability (i.e., better selectivity) (target area in Figure 10b). The selectivity, which is the ratio of proton conductivity to methanol permeability, is often used to evaluate the potential performance of DMFC membranes. The relative selectivities of copolymers are higher than that of Nafion as listed in Table 4.

Microstructure of the Membranes. Two-phase separated morphology has been observed in the microstructure of Nafion as well as some multiblock sulfonated copolymers and some PEMs containing densely and locally sulfonated acid sites.[6,7,42] Proton conductivity and dimensional stability of the membranes are closely related to their morphology. Wide proton-conducting channels formed by hydrophilic domains are helpful to the movement of protons but are possibly detrimental for mechanical properties and dimensional stability in hot water.[37] The typical microstructure of membranes SPAES-33 and SPAES-39 studied by TEM is shown in Figure 11. The bright and dark regions are derived from the hard segments corresponding to the hydrophobic units and the soft segments corresponding to the hydrophilic units containing water, respectively. Both SPAES-33 and SPAES-39 showed well-defined nanophase-separated structures and hydrophilic domains, which are indicated as the darker regions, were well-interconnected. The narrow and interconnected ionic channels (~2−5 nm) are believed to assist the proton conduction and be beneficial in improving the dimensional stability of membranes SPAES-33 and SPAES-39.

■ CONCLUSIONS

A novel fluorene-based bisphenol monomer containing four methoxy groups has been successfully synthesized in high yield by a facile phenol condensation reaction. Sulfonated poly(arylene ether sulfone)s (SPAES) with four pendant aliphatic sulfonic acid groups were obtained by sequential polycondensation, methoxy conversion, and sulfobutylation. In comparison with other representative SPAES structures and with Nafion

membranes, these membranes exhibited very low water uptake and dimensional change, even at elevated temperatures (80 °C). Anisotropic swelling of the present aliphatic side-chain fluorene-based SPAES was observed, which was greater in the through-plane direction than in the in-plane direction. The SPAES-36 and SPAES-39 membranes displayed good proton conductivity, which were comparable to or even higher than that of Nafion at ≥50% RH. It appears that the unique nanophase separation architecture and interconnected narrow ionic channels (∼2−5 nm) of both SPAES-33 and SPAES-39 are responsible for the high proton conductivities and low dimensional swelling. Moreover, the methanol permeability values of these SPAES membranes are much lower than Nafion. The combination of facile synthetic routes for monomer and polymers, good relative proton and methanol transport, and relatively low water uptake and swelling ratio makes these membranes attractive as PEM materials for further investigation in fuel cell applications.

AUTHOR INFORMATION

Corresponding Author

*E-mail: ymlee@hanyang.ac.kr; michael.guiver@nrc-cnrc.gc.ca.

Notes

[†]NRCC No. 53026.

ACKNOWLEDGMENT

Funding for the project by the WCU program, National Research Foundation (NRF) of the Korean Ministry of Science and Technology (No. R31-2008-000-10092-0) is gratefully acknowledged.

REFERENCES

(1) Carrette, L.; Friedrich, K. A.; Stimming, U. *Fuel Cells* **2001**, *1*, 5–39.
(2) Costamagna, P.; Srinivasan, S. *J. Power Sources* **2001**, *102*, 253–269.
(3) Hickner, M. A.; Ghassemi, H.; Kim, Y. S.; Einsla, B. R.; McGrath, J. E. *Chem. Rev.* **2004**, *104*, 4587–4611.
(4) Rikukawa, M.; Sanui, K. *Prog. Polym. Sci.* **2000**, *25*, 1463–1502.
(5) Peckham, T. J.; Holdcroft, S. *Adv. Mater.* **2010**, *22*, 4667–4690.
(6) Higashihara, T.; Matsumoto, K.; Ueda, M. *Polymer* **2009**, *50*, 5341–5357.
(7) Park, C. H.; Lee, C. H.; Guiver, M. D.; Lee, Y. M. *Prog. Polym. Sci.* **2011**, *36*, 1443–1498.
(8) Fujimoto, C. H.; Hickner, M. A.; Cornelius, C. J.; Loy, D. A. *Macromolecules* **2005**, *38*, 5010–5016.
(9) Wu, S. Q.; Qiu, Z. M.; Zhang, S. B.; Li, Z. Y. *Polymer* **2006**, *47*, 6993–7000.
(10) Xing, P.; Robertson, G. P.; Guiver, M. D.; Mikhailenko, S. D.; Wang, K.; Kaliaguine, S. *J. Membr. Sci.* **2004**, *229*, 95–106.
(11) Gao, Y.; Robertson, G. P.; Guiver, M. D.; Wang, G. Q.; Jian, X. G.; Mikhailenko, S. D.; Li, X.; Kaliaguine, S. *J. Membr. Sci.* **2006**, *278*, 26–34.
(12) Shang, X.; Tian, S.; Kong, L.; Meng, Y. *J. Membr. Sci.* **2005**, *266*, 94–101.
(13) Wang, F.; Hickner, M.; Kim, Y. S.; Zawodzinski, T. A.; McGrath, J. E. *J. Membr. Sci.* **2002**, *197*, 231–242.
(14) Chikashige, Y.; Chikyu, Y.; Miyatake, K.; Watanabe, M. *Macromolecules* **2005**, *38*, 7121–7126.
(15) Schuster, M.; Kreuer, K. D.; Andersen, H. T.; Maier, J. *Macromolecules* **2007**, *40*, 598–607.
(16) Bai, Z.; Dang, T. D. *Macromol. Rapid Commun.* **2006**, *27*, 1271–1277.
(17) Phu, D. S.; Lee, C. H.; Park, C. H.; Lee, S. Y.; Lee, Y. M. *Macromol. Rapid Commun.* **2009**, *30*, 64–68.
(18) Gao, Y.; Robertson, G. P.; Guiver, M. D.; Mikhailenko, S. D.; Li, X.; Kaliaguine, S. *Macromolecules* **2005**, *38*, 3237–3245.
(19) Wang, F.; Hickner, M.; Ji, Q.; Harrison, W.; Mecham, J.; Zawodzinski, T. A.; McGrath, J. E. *Macromol. Symp.* **2001**, *175*, 387–395.
(20) Genies, C.; Mercier, R.; Sillion, B.; Cornet, N.; Gebel, G.; Pineri, M. *Polymer* **2001**, *42*, 359–373.
(21) Miyatake, K.; Zhou, H.; Matsuo, T.; Uchida, H.; Watanabe, M. *Macromolecules* **2004**, *37*, 4961–4966.
(22) Yin, Y.; Suto, Y.; Sakabe, T.; Chen, S.; Hayashi, S.; Mishima, T.; Yamada, O.; Tanaka, K.; Kita, H.; Okamoto, K.-I. *Macromolecules* **2006**, *39*, 1189–1198.
(23) Li, N.; Cui, Z.; Zhang, S.; Li, S. *J. Polym. Sci., Part A: Polym. Chem.* **2008**, *46*, 2820–2832.
(24) Park, C. H.; Lee, C. H.; Sohn, J. Y.; Park, H. B.; Guiver, M. D.; Lee, Y. M. *J. Phys. Chem. B* **2010**, *114*, 12036–12045.
(25) Li, N.; Zhang, S.; Liu, J.; Zhang, F. *Macromolecules* **2008**, *41*, 4165–4172.
(26) Kreuer, K. D. *J. Membr. Sci.* **2001**, *185*, 29–39.
(27) Norsten, T. B.; Guiver, M. D.; Murphy, J.; Astill, T.; Navessin, T.; Holdcroft, S. *Adv. Funct. Mater.* **2006**, *16*, 1814–22.
(28) Lafitte, B.; Puchner, M.; Jannasch, P. *Macromol. Rapid Commun.* **2005**, *26*, 1464–1469.
(29) Pang, J. H.; Zhang, H. B.; Li, X. F.; Ren, D. F.; Jiang, Z. H. *Macromol. Rapid Commun.* **2007**, *28*, 2332–2338.
(30) Zhang, Y.; Wan, Y.; Zhao, C. J.; Shao, K.; Zhang, G.; Li, H. T.; Lin, H. D.; Na, H. *Polymer* **2009**, *50*, 4471–4478.
(31) Shao, K.; Zhu, J.; Zhao, G. J.; Li, X. F.; Cui, Z. M.; Zhang, Y.; Li, H. T.; Xu, D.; Zhang, G.; Fu, T. Z.; Wu, J.; Na, H.; Xing, W. *J. Polym. Sci., Part A: Polym. Chem.* **2009**, *47*, 5772–5783.
(32) Gao, L.; Zhang, F.; Zhang, S. B.; Liu, J. *J. Membr. Sci.* **2011**, *372*, 49–56.
(33) Yin, Y.; Yamada, O.; Suto, Y.; Mishima, T.; Tanaka, K.; Kita, H.; Okamoto, K. *J. Polym. Sci., Part A: Polym. Chem.* **2005**, *43*, 1545–1553.
(34) Asano, N.; Aoki, M.; Suzuki, S.; Miyatake, K.; Uchida, H.; Watanabe, M. *J. Am. Chem. Soc.* **2006**, *128*, 1762–1769.
(35) Li, N. W.; Shin, D. W.; Hwang, D. S.; Lee, Y. M.; Guiver, M. D. *Macromolecules* **2010**, *43*, 9810–9820.
(36) Li, Z.; Ding, J. F.; Robertson, G. P.; Guiver, M. D. *Macromolecules* **2006**, *39*, 6990–6996.
(37) Kim, D. S.; Robertson, G. P.; Guiver, M. D. *Macromolecules* **2008**, *41*, 2126–2134.
(38) Matsumura, S.; Hlil, A. R.; Lepiller, C.; Gaudet, J.; Guay, D.; Hay, A. S. *Macromolecules* **2008**, *41*, 277–280.
(39) Matsumura, S.; Hlil, A. R.; Lepiller, C.; Gaudet, J.; Guay, D.; Shi, Z. Q.; Holdcroft, S; Hay, A. S. *Macromolecules* **2008**, *41*, 281–284.
(40) Matsumoto, K.; Higashihara, T.; Ueda, M. *Macromolecules* **2009**, *42*, 1161–1166.
(41) Matsumoto, K.; Higashihara, T.; Ueda, M. *J. Polym. Sci., Part A: Polym. Chem.* **2009**, *47*, 3444–3453.
(42) Li, N. W.; Hwang, D. S.; Lee, S. Y.; Liu, Y. L.; Lee, Y. M.; Guiver, M. D. *Macromolecules* **2011**, *44*, 4901–4910.
(43) Miyatake, K.; Chikashige, Y.; Higuchi, E.; Watanabe, M. *J. Am. Chem. Soc.* **2007**, *129*, 3879–3887.
(44) Bae, B.; Miyatake, K.; Watanabe, M. *Macromolecules* **2010**, *43*, 2684–2691.
(45) Bae, B.; Yoda, T.; Miyatake, K.; Uchida, H.; Watanabe, M. *Angew. Chem., Int. Ed.* **2010**, *49*, 317–319.
(46) Aoki, M.; Chikashige, Y.; Miyatake, K.; Uchida, H.; Watanabe, M. *Electrochem. Commun.* **2006**, *8*, 1412–1416.
(47) Shang, X. Y.; Li, X. H.; Xiao, M.; Meng, Y. Z. *Polymer* **2006**, *47*, 3807–3813.
(48) Liu, B. J.; Hu, W.; Robertson, G. P.; Guiver, M. D. *J. Mater. Chem.* **2008**, *18*, 4675–4682.
(49) Liu, B. J.; Kim, D. S.; Murphy, J.; Robertson, G. P.; Guiver, M. D.; Mikhailenko, S.; Kaliaguine, S.; Sun, Y. M.; Liu, Y. L.; Lai, J. Y. *J. Membr. Sci.* **2006**, *280*, 54–64.

(50) Kim, Y. S.; Einsla, B.; Sankir, M.; Harrison, W.; Pivovar, B. S. *Polymer* **2006**, *47*, 4026–4035.
(51) Dimitrov, I.; Jankova, K.; Hvilsted, S. *J. Polym. Sci., Part A: Polym. Chem.* **2008**, *46*, 7827–7834.
(52) Liu, B. J.; Robertson, G. P.; Kim, D. S.; Guiver, M. D.; Hu, W.; Jiang, Z. H. *Macromolecules* **2007**, *40*, 1934–1944.